Polycaprolactone and Polyethylene Terephthalate Nanofiber Grafts for Anterior Cruciate Ligament Tissue Applications

Francisco Eliseo Jaramillo Torres, Bachelor in Biomedical Engineering

Submitted in fulfillment of the requirements for the degree of Master of Science in Biomedical Engineering

School of Engineering and Digital Sciences

Department of Chemical and Materials Engineering

Nazarbayev University

53 Kabanbay Batyr Avenue,
Nur-Sultan, Kazakhstan, 010000

Supervirsors:
Lead Supervisor Name: Associate Professor Cevat Erisken
Co-supervisor Name: Assistant Professor Dana Akilbekova

April 2024

DECLARATION

I hereby, declare that this manuscript, entitled "*Polycaprolactone and Polyethylene Terephthalate Nanofiber Grafts for Anterior Cruciate Ligament Tissue Applications",* is the result of my own work except for quotations and citations which have been duly acknowledged.

I also declare that, to the best of my knowledge and belief, it has not been previously or concurrently submitted, in whole or in part, for any other degree or diploma at Nazarbayev University or any other national or international institution.

Name: Francisco Jaramillo

Date: 08.04.2024

Abstract

One of the main ligaments which maintains the stability and prevents hyperextension of the knee joint during the articulations is the anterior cruciate ligament (ACL) is. Moreover, ACL is commonly broken during high-impact sports. If left untreated, this injury can result in complications, including inflammation and dislocation. Furthermore, ACL lacks of vascularity which is translated into poor self-healing. ACL repair surgery, utilizing allograft or autograft tissue, is the primary therapy for ACL injuries. However, ACL repair surgery has several disadvantages that might arise from the donor site include morbidity, extended recovery periods, and limited range of motion. To overcome secondary effects of ACL surgery reconstruction, tissue engineering has become a viable substitute. The current alternative for allograft or autograft is a synthetic graft made of biopolymers that can mimic the properties of ACL tissue and can be biodegradable and biocompatible with human body.

The present study hypothesizes that the produced graft from two different polymers (PCL&PET) with aligned-bimodal and unaligned-unimodal fibers can mimic the properties of healthy and injured ACL rabbit's tissue, respectively. To observe if the created graft is useful to replicate the conditions for ACL restoration, primary fibroblast taken from rabbit's ACL tissue were seeded on two different types of scaffolds: aligned fibers which represent healthy ACL tissue and unaligned which represent injured ACL tissue. After cell seeding, the evaluation of the cells proliferation and DNA was evaluated in 3 time points from day 0 to day 7.

Acknowledgements

I want to express my appreciation to all who accomplished the present study. Initially, I want to express my appreciation to my thesis advisor, Dr. Cevat Erisken, for his assistance, patience, encouragement, and guidance through the process of editing, managing, and organizing this research study. With his expertise and leadership, this study was possible. Secondly, I would want to convey my gratitude to my co-supervisor, Dr. Dana Akilbekova for her mentorship and suggestions that have greatly enhanced the quality of this research. Moreover, I want to thank the Biomaterials and Interface Regenerative Engineering Laboratory (BIREL) team, who contributed with their support and assistance to conduct all the experimental parts of this research. Their feedback, support and encouragement motivate me to make possible this study. I also want to express my gratitude to Dr. Yulia Safarova from the Laboratory of Bioengineering and Regenerative medicine, who helped me to conclude this study by mentoring me about cell cultures and how to manage the experiments in-vitro. Lastly, I want to convey my appreciation to my family and friends. Without their love, encouragement, and support, I would not have achieved my current position or developed into the person I am today. This thesis is dedicated to my mother, Monica Torres, who supported and encouraged me throughout my life and in every decision I made. I know that I have consistently received and will continue to receive her boundless affection.

Table of contents

List of Abbreviations & Symbols

AA Acetic Acid

ACL Anterior Cruciate Ligament

COL Collagen

DCM Dichloromethane

DMEM Dulbecco's Modified Eagle Medium

ECM Extracellular matrix

FA Formic Acid

FOV Field of View

GAG Glycosaminoglycan

PCL Poly(caprolactone)

PET Polyethylene terephthalate

PYR Pyridine

SEM Scanning Electron Microscopy

TEM Transmission Electron Microscopy

TFA Trifluoroacetic acid

List of Tables and Figures

CHAPTER 1 - INTRODUCTION

1.1.1 Ligament structure and composition

The composition of ligament tissue encompasses an extracellular matrix (ECM) and cellular components, comprising elastin, collagen, peptides and proteoglycans [1]. The ligament possesses a restricted number of cells, mainly consisting of ligamentocytes and ligamentoblasts, which make up around 95% of the cellular composition [2]. There are also smaller amounts of bone marrow, synovial, and vascular cells. Ligament cells are significant in tissue development and remodeling. They can react to stimuli and adjust to their surroundings in situations involving stresses and strains [3].

Collagen makes up the majority of the anterior cruciate ligament (ACL), accounting for approximately 60%. Moreover. collagen is predominantly made up of collagen type I, which makes up about 95% of the total content, and around 85% of the mass of the ECM is composed of dry weight. The remaining 5% comprises COL type III and COL type V. Furthermore, the ordered arrangement of the ligament is mainly constituted by collagen [4].

The ligament's structure is formed by the tropocollagen molecule, which is produced inside cells and then released as procollagen in the ECM [5]. When molecules aggregate, they form a fibril, the primary nano-structural entity. The diameter of these fibrils can range from 20 to 150 nanometers. The fibers of collagen are produced from a cluster of filaments measuring about one micrometer in diameter. [6]. A collection of fibers creates an essential package known as the sub-fascicle, which subsequently gives rise to a secondary bundle called the fascicle [7]. Finally, a third package of fibrils with a diameter ranging from 500 to 1000 micrometers contributes to the formation of the ligament. The endo ligament, a thin collagen layer, envelops the collagen fibers and encompasses neurons, blood vessels, and lymphatic vessels [8].

1.1.2 Anterior cruciate ligament

The ACL is a crucial component of the knee joint, which regulates the range of motion and offers stability during articulations. This ligament is one of the four main connectors between the the tibia and femur [9]. The ACL primarily functions to restrict excessive extension of the knee joint by controlling the forward movement of the tibia with respect to the femur. This ligament is

essential for supporting sudden stops, changes in direction, and abrupt movements, which are common in sports such as soccer, basketball, and skiing [10].

Despite its significance, the ACL is prone to damage, which frequently happens when engaging in motions that require sudden stops, sharp turns, or direct hits to the knee. ACL tears can cause severe pain, edema, and instability in the knee joint. In the United States, ACL ruptures count more than two hundred thousand annually, often leading to debilitating joint instability and osteoarthritis [11]. Furthermore, if this rupture is not treated on time, it can lead to several problems, such as inflammation and dislocation. Depending on the severity of the injury, there are many ways to treat ACL, from conventional procedures like physical therapy to surgical repair [10]. After an ACL injury, patients usually need a thorough rehabilitation program to rebuild their knee's strength, flexibility, and function.

Because of the limited blood supply to the ACL, its healing process is often slow, the most used treatment for ACL injuries is reconstruction surgery using either allograft, autograft, or synthetic tissue [12]. Even though using autografts is generally considered the best option for replacing the ACL, there are several drawbacks, including longer recovery times, morbidity at the donor site, and a constrained range of motion [13]. Therefore, an effective technique for ACL regeneration has been developed using tissue engineering. For an ACL injury to be effectively Repaired, engineered tissue must have the same biomechanical and physiological characteristics as the native ACL tissue.

1.2.1 Polymer process for scaffold production

There are several techniques to process the polymer to produce scaffolds in tissue engineering, including 3D bioprinting, salt leaching, gas foaming, fiber deposition, and electrospinning [14]. In the case of ACL, it is necessary to obtain aligned fibers with nanometric diameters. While several techniques are available for creating fibrous scaffolds, electrospinning represents a versatile and innovative technique to develop ultrafine fibers with different sizes varying from nanometers up to micrometers [15]. The procedure of electrospinning entails introducing a conductive solution of polymers. On one side, there's a spinneret, while on the other side, there's a collector. Understanding the role of electrical potential difference is essential in the

formation of fibers. It effectively counteracts the surface tension of the polymer droplet, guiding the fiber jet downstream and causing its diameter to decrease. [16].

One of the valuable advantages of electrospinning lies in its ability to produce nanofibrous structures that may mimic the extracellular matrix of biological tissues, providing a scaffold for cell growth and regeneration. Other advantages related to the electrospinning method are the ease of fabrication, the fact that it is not expensive, and the capability to manipulate the width of the fiber [17]. This makes electrospinning particularly valuable in tissue engineering applications, where creating biomimetic scaffolds is decisive for supporting cell adhesion, proliferation, and differentiation. Moreover, the process offers precise control over the morphology, porosity, and composition of the resultant nanofibers, allowing researchers to tailor the properties of the materials to meet specific requirements [18].

1.2.2 The impact of fiber diameter

The composition of ligament tissue consists of collagens with varying sizes ranging from 10 nm to 1 μm. According to Jenkins & Little, the regulation of cell differentiation is mainly influenced by fiber diameter [19]. In the human rotator cuff investigation, fibroblasts were introduced onto scaffolds of nanofibrous PLGA with dimensions of 320 nanometers, 680 nanometers, and 1.80 μm [20]. After 28 days, the findings suggested that the cells presented a higher degree of alignment on the thicker fibers as opposed to the thinner ones. A greater fiber diameter promotes cellular elongation and the development of a spindle-like morphology. Aligned fibers promote fibroblast expansion and differentiation, regardless of their diameter.

In contrast, small-diameter fibers exhibited a considerably larger cell number than the large-diameter groups [19]. Furthermore, fibroblasts in thinner fibers exhibited higher collagen and proteoglycan production in tendon tissue, which shares a similar structure with ligament. Specifically, they produced around 0.75 wt% and 0.036 wt% of collagen and proteoglycans on fiber of 320 nanometer, compared to 0.023wt% and 0.64 wt% on fiber of 1.80 micrometer. Additionally, these fibroblasts facilitated a more muscular deposition of proteoglycans. It was hypothesized that the thinner nanofibers, which mimic the structure of wounded tendon tissue, enhance the cells' ability to generate additional components of the matrix.

In contrast, large nanofibers produce an apparent resemblance to a strong tendon, preventing cells from synthesizing excessive collagen and proteoglycan [20]. Nevertheless, while

analyzing biomarker expression, COL I, COL III, COL IV and tenomodulin showed the maximum levels within the scaffold, possibly due to decreased production of collagen.

The strong resemblance to the original structure is crucial because of the inadequate rearrangement of collagen fibrils in the wounded tissue [6]. Given that ECM composites are characterized by their nanometer scale, producing materials with nanoscale architectures that accurately replicate tissue characteristics is imperative. Nanofibers are the most often utilized nanostructures [21]. These fibers are fragile and linked, providing many holes of different sizes. This gives cells enough surface area to bind to them and allows for the free flow of nutrients.

1.2.3 Cell source for the scaffold

Although it is crucial to utilize a suitable cell type in order to get a functioning ligament construct, there is limited knowledge regarding the most effective cell source. There are different options to consider, such as primary fibroblasts or mesenchymal stem cells (MSC) that can be sourced from ligaments like the medial collateral ligament (MCL) or ACL. In a recent study, Ge et al. examined the effectiveness of fibroblasts obtained from the MCL and ACL in rabbits, comparing them to MSCs derived from bone marrow. The researcher observed that the rate of cell division and the generation of collagen were more significant when using MSCs compared to fibroblasts. The study found that MSCs have the potential to be a more effective cell source than MCL and ACL fibroblasts for remodeling anterior cruciate ligament tissue. [22]. Moreover, when cultured on silk scaffolds, Liu et al. observed that MSCs exhibited better growth rates than fibroblasts. Additionally, there was a notable difference in the production and expression of genes between the fibroblast and MSC groups. [23]. In contrast, recent research finding indicate that acellular collagen scaffold implants have demonstrated remarkable efficacy in promoting tissue growth and effectively recovering rabbit Achilles tendon or ACL, showing comparable performance for autografts. Furthermore, in research conducted by Dunn et al., they discovered that fibroblast-seeded collagen scaffolds exhibited potential for ACL reconstruction, where ACL fibroblasts demonstrated a higher level of adhesion compared to other fibroblasts. [24].

In the present research work was planned to use primary fibroblast from rabbit’s ACL and seed them into the polymeric membrane composed of PET&PCL, to evaluate the performance of the scaffolds with seeded fibroblasts.

1.3 Biomaterials selection

Ligament regeneration biomaterials may be categorized into two main types: natural polymers and synthetic polymers. Various types of scaffolds are commonly created using a range of natural and synthetic polymers. Natural polymers like collagen, hyaluronic acid (HA), gelatin and chitosan are often utilized alongside synthetic polymers like PLGA, polyethylene terephthalate, polyglycolide and polycaprolactone [2]. While biomaterials derived from natural polymers promote accelerated cell growth, they undergo quick degradation, possess limited mechanical strength, and face difficulties treating latent immunogenicity [25]. Synthetic materials are more flexible and frequently employed due to their advantageous properties. They are cost-effective, can be synthesized in significant amounts and can regulate the rate at which they degrade. Nevertheless, their bioactivity is reduced, and the degradation products that arise can be harmful. [3]. Moreover, poly-L-lactic acid, polycaprolactone, polyethylene terephthalate, and polyglycolic acid are the most used synthetic polymers. One significant advantage of synthetic polymers is their versatility in obtaining them through various methods, while a significant drawback is the potential for inflammatory reactions caused by degradation products [7]. Biocompatible biomaterials are preferred in most applications due to their minimal immune reaction.

Biomaterials can be composed of either electrospun or woven fibers in structure. Also, woven scaffolds provide the advantage of having an interconnected porous structure, but cell seeding and proliferation processes within these systems can be pretty complex. Electrospun fiber-based scaffolds possess exceptional cell adhesion properties due to their remarkable characteristics, such as excellent permeability, optimal surface-to-volume ratio, and adjustable pore size [5]. Additionally, the fibers enable the replication of the original extracellular matrix (ECM) structure and enhance the material's tensile characteristics by manipulating fiber diameter and arrangement [1]. Fibrous scaffolds are commonly preferred and extensively utilized due to their ability to closely resemble the natural tissue structure and the fibrous nature of ligaments. The utilization of nanofibers has been extensively investigated in the context of repairing various musculoskeletal tissues, such as ligaments, tendons, meniscuses, cartilage, intervertebral disks, and bones[4].

The present research study aimed to produce synthetic scaffolds by merging two different polymers, polycaprolactone (PCL) and polyethylene terephthalate (PET), to achieve the best possible scaffold that replicates the natural biomechanical characteristics of the ACL and is compatible with living organisms. PCL and PET possess different properties and, combined, can lead to obtaining a resistant and biocompatible material to be used as a graft for ACL reconstruction.

1.3.1 Polycaprolactone (PCL)

Polycaprolactone (PCL) is frequently utilized in the creation of scaffolds for tissue engineering due to its excellent structural stability biocompatibility, impressive mechanical properties, and biodegradability. This synthetic polymer is known for its remarkable flexibility, low melting point, and exceptional biocompatibility [11]. PCL has gradual degradation kinetics, making it suitable for extended uses. PCL's main benefit is its adaptability for processing since it can be melted and molded into different forms or spun into fibers by methods such as electrospinning. One common application of PCL is in the creation of scaffolds for tissue regeneration and controlled drug release systems because of its biodegrading capacity and compatibility with human tissues [9]. PCL's capacity to offer structural support during tissue healing and its progressive degradation into harmless byproducts renders it a promising material for creating implanted medical devices and structures that facilitate the regeneration of injured tissues.

1.3.2 Polyethylene terephthalate (PET)

Prosthetic grafts have widely adopted polyethylene terephthalate (PET) because of its impressive mechanical strength and excellent biocompatibility. This linear polyester is known for its exceptional mechanical properties and finds extensive use in the biomedical industry. It is not biodegradable, but its durability makes it highly valuable [26]. Moreover, the nonwoven PET matrices possess porosity, significant surface area, and interconnected pores, which greatly enhance mass transfer efficiency and allow for higher cell concentrations [27].

PET is utilized in engineering components, medical devices, and diverse industrial sectors because of its advantageous qualities and compatibility with different production methods [28].

Furthermore, PET has been extensively reported to be a nondegradable material employed for in vitro cell culture to maintain the cell culture environment constant during tissue regeneration. However, PET has strong hydrophobicity that limits its applicability [29]. For the reasons mentioned above, it is necessary to combine PET with other polymer such as PCL to enhance the material properties that can lead to obtain a material which can mimic the native ACL tissue.

Table 1 summarizes the previous research made in ACL grafts, which includes different materials used and parameters to evaluate the mechanical properties of the produced grafts.

Material	**Diameter distribution**	**rate**	**Load - stress - Modulus**		**Time after implantation**	**Reference**
			Native Tissue	**Graft**		
PLLA/PET (20/4) yarns	Braided yarns	12 mm/min	Load 440,1 N Stiffness 178.5 N/mm	Load 384,5 N Stiffness 193,3 N/mm	12 weeks	[30]
PCL/PET (15-layer coating PCL film+PET woven sheet)	No reference	5 mm/min	No reference	Load 101.9 + 8.1 N Stiffness 28.7 ± 2.0 N/mm	6 & 12 weeks	[31]
PCL/nHAp/Col	Randomly aligned	2 mm/min	No reference	Load 58.4±4.1 N Stiffness 15.2±1.4N/mm	4 & 12 weeks	[32]
PCLF-PET	No reference	20 mm/min	Load 353 ± 33 N	Load 72 ± 30 N Load 40 ± 34 N	8 weeks	[33]
PET/HA	No reference	2 mm/min	No reference	Load 70.67±5.48 N Load 78.03±6.60 N Stiffness 26.40±1.84 N/mm Stiffness 31.17±2.49 N/mm	8 & 12 weeks	[34]

Table 1. Comparison of ACL grafts using different polymers and parameters.

For the development of new ligament tissue, it is crucial to find the ideal matrix for ACL regeneration must be porous, biodegradable, and strong enough mechanically. Combining degradable and non-degradable scaffolds loaded with cells will produce better results than scaffolds without cells [31]. It is proposed to combine different polymers, such as PET/PCL, functionalized with primary rabbit ACL cells to have a strong composite that can replicate the characteristics of a natural ACL and stress forces. Reconstruction surgery using either autograft or

allograft means risks of infection, re-rupture, decreased mobility at the donor site (autograft), and other complications [9]. In this context, tissue engineering offers a therapeutic strategy to address ACL lesions by integrating and transferring specific structural characteristics from the original ACL to the graft.

The present research aims to create a biomimetic graft by electrospinning it and shed light on its potential as a therapeutic option in vitro. The aims of this project will be achieved by using the electrospinning technique to fabricate synthetic scaffolds, evaluate the biomechanical characteristics of the graft, use different polymer materials, and seed primary ACL fibroblasts into the scaffolds to assess cell proliferation in vitro. As mentioned before, ACL injuries are the most common problem worldwide, and the traditional methods to repair ACLs depict low-quality restoration, leading to several problems. Several studies have tried with different polymers, such as polycaprolactone by electro-spun, but showed limited results as they did not combine with ACL fibroblast or other polymers [16].

1.4 Problem statement, objectives, and research hypothesis.

The ACL cannot mend itself after being torn or ruptured because of its low blood supply and dynamic characteristics. The current gold standard treatment for ACL injuries involves restoration utilizing allografts. However, this alternative may result in increased illness at the donor site, reduced moving range, a higher danger of re-fracture, and the possibility of infection. We need to find a more sustainable approach to recovering torn ACLs. Moreover, tissue engineering utilizes biomaterials to create scaffolds or grafts that mimic the structural features of the original ACL tissue, providing a solution for ACL injuries. It is hypothesized that by using a scaffold made by bimodal diameter distribution with aligned PET and PCL nanofibers, we can accurately replicate the varying sizes of collagen fibrils found in the rabbit's ACL. This replication will allow us to mimic the biomechanical characteristics of ACL tissue and create a suitable environment for cell growth and attachment using primary rabbit ACL cells. This research aims to develop biomimetic ACL scaffolds utilizing various polymer compositions, specifically PET and PCL, to reproduce the fiber distribution and mechanical properties of ACL tissue found in rabbits and also seed fibroblast ACL cells to evaluate cell distribution, fiber alignment, and cell growth in the scaffolds.

The research aims to achieve the following objectives:

1. **Evaluation of Biomechanical Properties**: To compare biomimetic grafts to conventional graft materials in a rabbit ACL tissue regarding their biomechanical qualities, such as tensile strength, stiffness, and load-bearing capacity.
2. **Histological Analysis**: To perform a histological analysis of the graft site to look at tissue regeneration, collagen deposition, and the presence of fibrous tissue in the graft, showing details about how the grafts are based on biology.
3. **Imaging and Microstructural Analysis**: To investigate the microstructure of the grafts, their integration into the host tissues, and any indications of graft deterioration or remodeling, advanced imaging methods like optical microscopy and scanning electron microscopy (SEM).
4. **Cell seeding:** Seed primary ACL fibroblasts into the scaffolds and evaluate their proliferation, collagen, GAG and DNA production.
5. **Comparative Analysis**: To evaluate the functional results, biomechanical characteristics, and biocompatibility of biomimetic grafts compared to traditional graft materials (such as autografts or allografts).
6. **Clinical Implications**: Consider whether biomimetic grafts are appropriate for ACL reconstruction in individuals and note any potential benefits or drawbacks to extrapolate the findings to potential clinical applications.
7. **Future Development and Optimization**: To provide insights for future research by identifying areas for improvement in biomimetic graft design and fabrication techniques, aiming to enhance their performance and clinical applicability.

Chapter 2 - Materials and Methods

Polymeric membrane reagents

Reagents used in these experiments include polycaprolactone (Sigma-Aldrich, UK, #440744), polyethylene terephthalate (USP, Rockville, MD, USA, #1546900), acetic acid (Sigma-Aldrich, St Louis, MO, USA, #270725), trifluoroacetic acid (Sigma-Aldrich, France, #302031), dichloromethane (Sigma-Aldrich, St Louis, MO, USA, #270997), formic acid (Merck KGaA, Darmstadt, Germany, #110854), and pyridine (Sigma-Aldrich, St Louis, MO, USA, #270970), DMEM/ nutrient mixture F-12 (1:1) (1x) (#2645233) (GIBCO) .

Cell seeding reagents

Trypan Blue Solution, Ascorbic Acid (AA) stock solution (50mg/mL), Dulbecco's Modified Eagle Medium (GIBCO, UK, 500Ml, #2436660), Fetal Bovine Serum, Dulbecco's Phosphate Buffered Saline (SIGMA-Aldrich, St. Louis, USA, RNBH3768), TrypLE (GIBCO, Denmark, #2472316)

1.1 Cell count & cell seeding

Below are the protocols for cell count and cell seeding:

Cell seeding:

- The cells were seeded (seeding volume=10µL) on the scaffolds and allowed cells to attach for 15 minutes in the incubator. Cell seeding density = 30,000/scaffold=3x104 cells/cm2.
- 2mL of fresh full supplemented DMEM were added (10% FBS, 1% P/S, 1% NEAA, 0.1% AMP-B, 0.1% GM + 50 µg/mL AA). 50mg/mL AA stock solution was prepared, filter sterilize, and added it to the media at the fused time (take 100µl from stock solution per 100mL of media).
- Incubated at 37C and 5% CO2. The media was changed twice a week.

Cell Count:

- the media was aspirated from cell culture flasks (BD Falcon, 600mL, Ref:355001)
- The flasks should be washed once with sterile PBS (10mL) and aspirated.

- 3 mL Trypsin EDTA, 1X (Trypsin, Mediatech Inc., Manassas, VA, Cat# 25-053-CI) , should be added to each flask and incubated for 3 minutes (at 37C and 5% CO2).
- 10mL of full supplemented DMEM should be added (10% FBS, 1% P/S, 1% NEAA, 0.1% AMP-B, 0.1% GM). The bottom surface of the flask should be washed while adding media and the surface should be rinsed thoroughly to detach any cells remaining on the surface.
- Transfer cell suspension into 50mL tubes, rinse the flask using 5mL sterile PBS and transfer the suspension to the tube. Note: Repeat the same procedure for other flasks and transfer the 3-4 flasks cells into the same 50 mL tube.
- Centrifuge (Fisher Scientific, Model 225, Cat#04-978-50) tube contents for 15 minutes at speed 3.5 and aspirate media.
- Add 3mL of fully supplemented DMEM (10% FBS, 1% P/S, 1% NEAA, 0.1% AMP-B, 0.1% GM) to one of the tubes and suspend the cells. Then, add the cell suspension into another tube containing cells-only and further suspend the contents of the two tubes merged.
- Merge the contents of two tubes into one as described above for the remaining tubes.
- For counting the cells, dilute 50µL of cell suspension with 50µL of Trypan Blue Solution (Mediatech, Inc, Herndon, VA, Cat# 25-900-CI) and vortex.
- Transfer 10µL of dilution into both sides of the Hemacytometer (Bright-line Hemacytometer, Hausser Scientific, Horsham, PA) and count the cell number in each of the four quadrants on each side. Then, take the average of all eight quadrants. Repeat this to have two readings per tube.
- Count the number of cells for the other tubes twice following the same procedure.
- If you are counting more than 150 cells in each quadrant, you may wish to dilute the cell suspension further to increase the precision and save time.
- Take the average of all and calculate the total number of cells in 1 mL of suspension by:

  (average count) x (dilution factor) x104 cells/mL.

Multiply this by the total volume to calculate the total number of cells

- Then, collect all the cells in a single tube, dilute or concentrate the cell suspension to have 30,000 cells in 10µL, suspend thoroughly, and keep in the incubator until seeding.

The grafts will be seeded and unseeded with primary rabbit ACL cells, first isolated and seeded to observe the differences between scaffolds, tissue infiltration, cell distribution, and cell growth.

1.3 Cell Proliferation

- The media from wells is aspirated.

-Rinsing with 1mL of PBS twice and aspirating follows.

-The backings are removed after the first rinse with no damage to the cell/scaffold construct.

-The weight of 1.5µL micro centrifuge tubes (Fisher Scientific, Cat# 05-408-129) is measured and recorded (Using tubes with flat bottom will create problems when sonicating the contents before the analysis).

-The scaffolds are dehydrated by being laid on both sides on a soft paper for 2-3s.

-The weight of tube + wet cell/scaffold is measured and recorded.

-1mL of 0.1% Triton X (Sigma, T-9284) is added and thoroughly vortexed for 1 min at the highest strength.

-Storage at -80° C (Storage at -30°C if doing DNA only) is done.

Picogreen dsDNA Quantfication

The picogreen dsDNA quantification reagent is a cynide dye optimized for dsDNA, with a high affinity for nucleic acids. It exhibits an extremely large fluorescence enhancement on binding. The detection limit ranges between 25pg/mL and 1000pg/mL with a standard spectrophotometer and fluorescein excitation (485 nm) and emission (535nm) wavelengths. As you are working, store everything on ice. Before reading, remove cover, remove bubbles and wipe condensation from the bottom of the plate.

Reagents:

- Reagent A':
- 39.8 mL Reagent B
- 200µL of Component-A of Picogreen dsDNA quantification kit (Invitrogen, Eugene, Oregon Product# P11496).
- Keep in dark (wrap aluminum foil)
- Regent B: TE (1X)
- 10mM Tris-HCl and 1 mM EDTA

Reagent C':

30 µL of Component-C (100µg/mL lambda) of Picogreen dsDNA quantification kit (Invitrogen, Eugene, Oregon Product# P11496).

1.47 mL Reagent B to dilute standard to 2µg/mL.

Sample:

Sonicate (Microson Model: XL-2000, Misonix Incorporated, Farmingdale, NY) samples in tubes with scaffolds and monolayers for 15s. Adjust the sonication intensity to indicator 2 and immerse the microprobe (tip diameter=1/8") close to the bottom of tubes for higher efficiency.

In each well, in the order indicated, add:

- 25 µL sample
- 75 µL Reagent B
- 100 µL Reagent A'
- Store at room temperature in the dark for 5 min.

Well#	Reagent B (µL)	Reagent C' (µL)	Reagent A' (µL)	DNA Concentration (ng/mL)
1	100	0	100	0
2	99.9	0.1	100	1
3	99.5	0.5	100	5
4	99	1	100	10
5	97.5	2.5	100	25
6	95	5	100	50
7	90	10	100	100
8	75	25	100	250
9	50	50	100	500
10	0	100	100	1000

Standard preparation: Two rows of standards suggested

After reading, correct for dilution (8-fold dilution from sample-200µm/25µm) and convert to number of cells assuming that each cell contains 8pg of DNA.

2. Fabrication of synthetic scaffolds

The synthetic scaffolds with aligned fibers possess a bimodal distribution and imitate the characteristics of native ACL. In contrast, the unaligned fibers have unimodal fiber distribution and simulate the injured ACL tissue. Moreover, before reaching the desired diameter distribution, many different polymeric concentrations were tested, such as PET 5% with PCL 8%, PCL 8%

with PET 5.5%, PET 4.5% and PET 6%, and finally PET 4.6% and PCL 8%. The synthesized scaffold needs to maintain an aligned fiber diameter similar to the native tissue, which ranges from 80-160 nm, while unimodal fiber distribution is around 100 nm. Moreover, the *in-vitro* study includes the synthetic grafts as experimental groups and natural ACL as the control group.

The electrospinning technique was employed to obtain the synthetic scaffolds (unimodal and bimodal distributions). For bimodal distribution, as shown in Figure 1 (A) the configuration of two syringes positioned oppositely with different polymer compositions, PCL 8% and PET 4.6%, was used to obtain different fiber diameters collected by a rotating drum in the middle of the syringes, which contained aluminum foil because it is conductive and attracted the fibers. As shown in figure 1 (B) both syringes were positioned on the same side for unaligned unimodal fiber distribution, and a collector plate was used instead of a rotator drum.

As shown in Table 2, to prepare PCL with a concentration of 8%, it was necessary to use 0.08 gr of PCL, 500 µl of acetic acid, 500 µl of formic acid and 6 µl of pyridine, then stir for 2 hours at 40°C. To prepare PET, 4.6% was necessary to use 0.046 grams of PET, 200 µl of TFA, 800 µl of DCM, and mixing for one hour at ambient temperature. Moreover, the optimal parameters employed to produce electrospun fibers were: PET 4.6% with one syringe with a flow rate of 0.09 ml/h, distance of 15 cm, voltage of 9 kV and rotation speed of 2000 rpm. The parameters employed for PCL 8% in 1 syringe, flow rate of 0.03 ml/h, distance of 7 cm, voltage of 9 kV and rotation speed of 2000 rpm.

As shown in table 3, the same method was used to prepare PCL 12% and PET 3.9%. The optimal parameters employed to produce electrospun fibers were: PET 3.9%, flow rate of 0.09 ml/h, distance of 20 cm, voltage of 16 kV and rotation speed of 2000 rpm and; PCL 8% in 1 syringe, flow rate of 0.09 ml/h, distance of 7 cm, voltage of 12 kV and rotation speed of 2000 rpm.

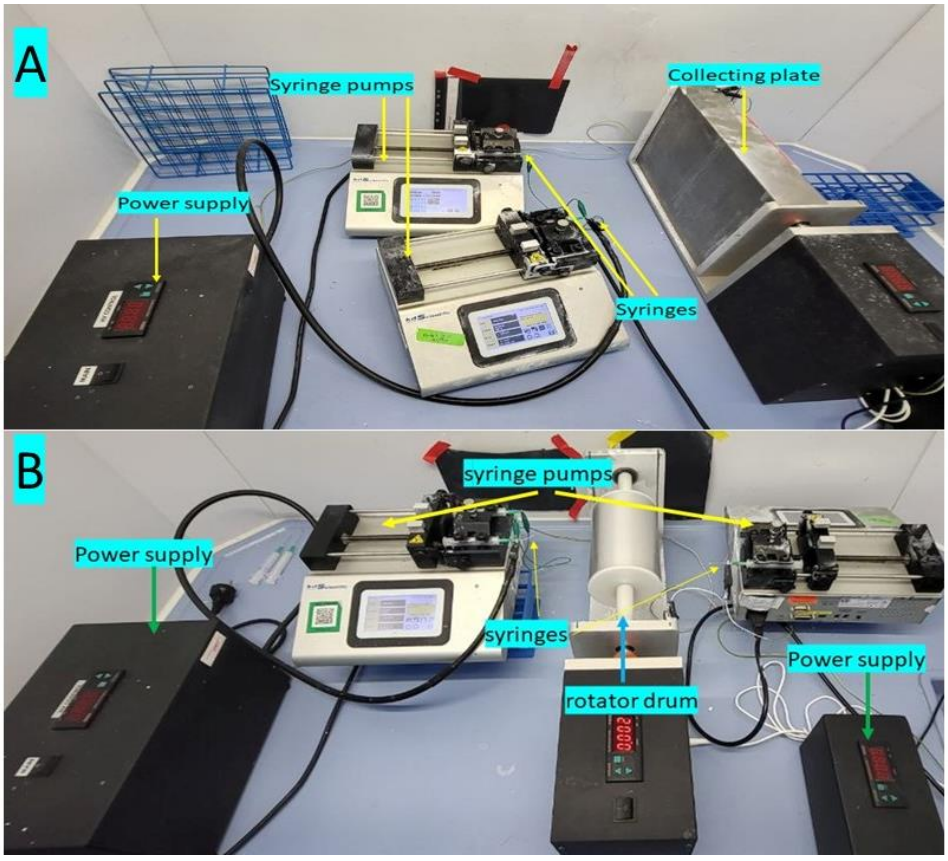

Figure 1. Picture of e-spinning set up for scaffold fabrication. A) aligned. B) unaligned

Aligned PCL&PET scaffold	**Solvents**						**Process Parameters**			
	Polymer (gr)	AA (µl)	DCM (µl)	FA (µl)	PYR (µl)	TFA (µl)	Distance (cm)	Drum speed (rpm)	Flow rate (ml/h)	Voltage (kV)
PCL 8%	0.08	500		500	6		7	2000	0.03	9
PET 4.6%	0.046		800			200	15	2000	0.09	9

Table 2. Formulation of the parameters to produce aligned scaffolds of PCL&PET

Unaligned PCL&PET scaffold		**Solvents**					**Process Parameters**			
	Polymer (gr)	AA (µl)	DCM (µl)	FA (µl)	PYR (µl)	TFA (µl)	Distance (cm)	Drum speed (rpm)	Flow rate (ml/h)	Voltage (kV)
PCL 12%	0.12	500		500	6		7	2000	0.09	12
PET 3.9%	0.039		800			200	20	2000	0.09	16

Table 3. Formulation of the parameters to produce unaligned scaffolds of PCL&PET

3. Mechanical test

The mechanical test was performed without cell seeding. The membranes of the polymers (PCL/PET) were used to evaluate the mechanical performance, and comparisons were made between the results and the biomechanical characteristics of native ACL from rabbits. A mechanical testing equipment (MTS Systems Co., Model 43, Eden Prairie, N, US) was used to apply a uniaxial force to deform the polymeric membranes. The membranes had a size of 4 cm, width of 10 mm, and thickness of 0.01 mm. Moreover, the membranes were strained uniaxially at a 5 mm/min deformation rate until the failure. Six tests were made for bimodal fiber membranes of PET 4.6% and PCL 8% (n=6), while eight tests were made for unimodal membranes of PET 8% and PCL 15% (n=4).

4. Microscopy characterization

Scanning electron microscope

After the fabrication of synthetic grafts, they were examined using SEM (JEOL JSM-IT200(LA)) at an accelerating voltage of 20 kV. Images were taken with different magnifications ranging from 2,000 to 15,000 augmentation. Moreover, Image J was used to analyze the diameter and establish the nanofibers' unimodal and bimodal distribution.

5. Statistical analysis

The study utilized a one-way analysis of variance (ANOVA) followed by the Tukey HSD (Honest Significant Difference) posthoc test to assess the mechanical characteristics of bimodal PCL/PET scaffolds, and a healthy ACL tissue. A non-paired student-t test was employed to examine and compare the collagen diameter of healthy ACL, the diameter of the fibers from PCL/PET scaffold, the diameter of the fibers of PCL scaffolds, and the biomechanical characteristics of PCL/PET and PCL scaffolds. A statistical difference was seemed significant when the p-value fell below the threshold of 0.05.

Chapter 3 - RESULTS

Diameter distribution and fiber alignment

Figure 2 presents the diameter distribution of the synthetic scaffolds, including both bimodal and unimodal distributions, and a comparison between healthy and injured ACL rabbit tissue accompanied by the respective graphs, TEM, and SEM images. As shown in Figure 2(A), the graph shows a bimodal fiber distribution in both cases, aligned fibers and healthy ACL tissue. In contrast, the unaligned fibers showed an unimodal diameter distribution of the fibers (Figure 2(C). Figure 2(B) represents the TEM and SEM for healthy ACL tissue and aligned PET/PCL scaffold. Figure 2(D) shows the TEM and SEM from injured ACL tissue and unaligned PET/PCL scaffold, respectively. Figure 2(E) presents the comparison table between the scaffolds and ACL tissue. On one side, the fiber distribution in healthy ACL tissue showed a bimodal pattern with two distinct peaks at 80 ± 0.0 nm and 160 ± 0.0 nm. At the same time, the fabricated aligned scaffold presented bimodal fiber distribution with two distinct points at 80 ± 6.4 nm and 160 ± 0.0 nm. On the other hand, injured ACL tissue presents one peak at 125 nm ± 19.1 nm, while an unaligned scaffold has one peak at 112 ± 11 nm.

Figure 3 showcases the comparison between healthy and injured ACL fibers and aligned and unaligned PET/PCL scaffolds. A sharp graph was seen in the aligned bimodal scaffolds, indicating the alignment of the scaffolds in Figure 3 (C). The scaffolds were made up of fibers aligned in a longitudinal manner, as indicated by a typical pattern of angles, with an average angle of 7.30°. (Figures 3(A1) and C). Random aligned unimodal scaffolds, in contrast, exhibit a uniform distribution of angles, indicating a departure from alignment Figure 3 (B, D). A notable difference was seen in the mean angle between aligned and unaligned fibers. The graphs of the PCL/PET scaffolds are similar to native ACL tissue, as seen in Figure 3 (C and D).

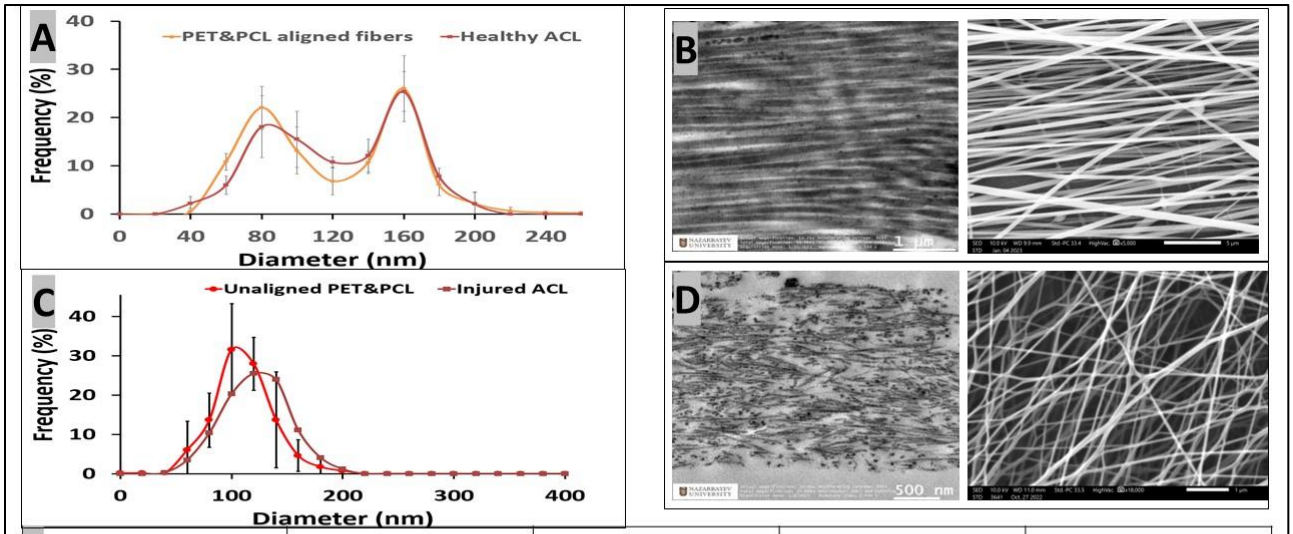

E Fibril diameter (nm)	Healthy ACL		Aligned PET&PCL		Injured ACL	Unaligned PET&PCL
Range	40-200		40-340		20-220	20-320
Peaks	80±6.4	160	80	160	125±19.1	112±11
Mean Diameter	113.5±2.4		116±8.7		112.4±10.1	110±14.4
Number Average Diameter	124.3±2.4		125.7±9.1		123.2±11.0	106.5±14.7

Figure 2. Diameter distributions. A) Frequency distribution of healthy rabbit ACL and PCL/PET aligned fibers. B) TEM image of healthy ACL and SEM image of aligned PET/PCL scaffold. C)Frequency distribution of injured rabbit ACL and PCL/PET unaligned fibers. D) TEM image of injured ACL and SEM image of unaligned PET/PCL scaffold. E) A table comparing A and C.

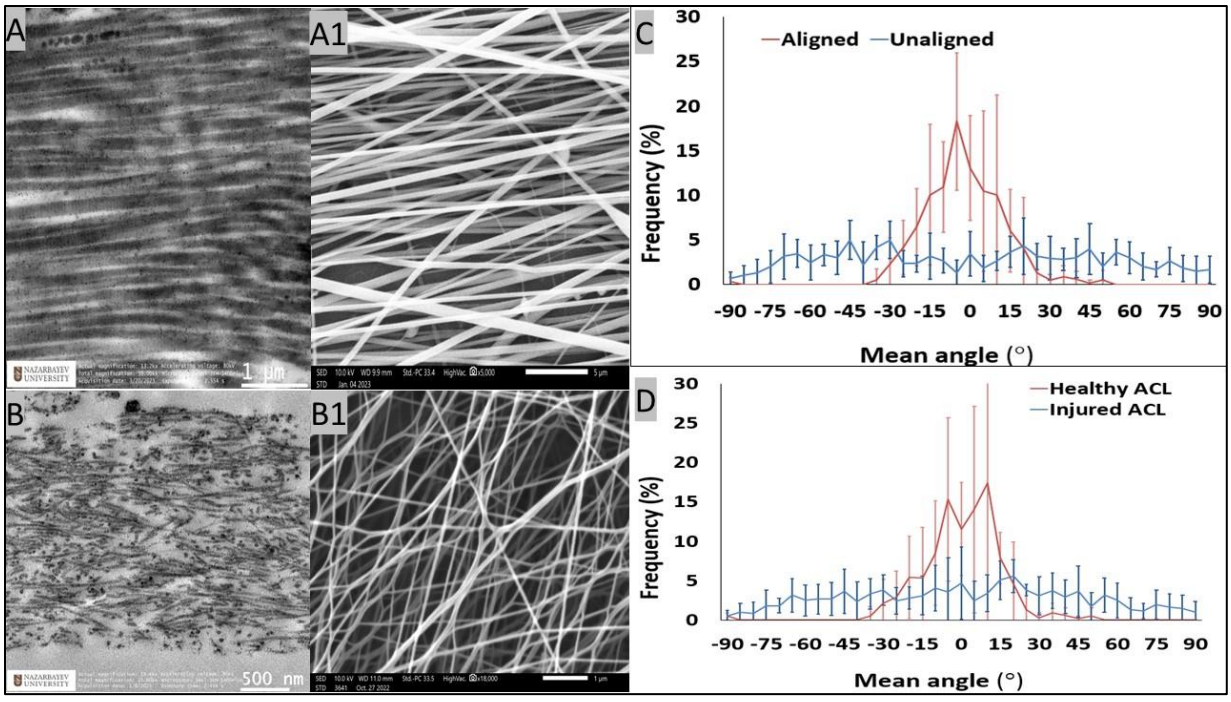

Figure 3. Alignment comparison between ACL and PCL/PET fibers. A) TEM and SEM of healthy ACL and aligned PET/PCL respectively (A1). B) TEM and SEM of injured ACL and unaligned PET/PCL (B1)

respectively. C) Graph of the mean angle and frequency between aligned and unaligned PET/PCL fibers. D) Graph of the mean angle and frequency between healthy and injured rabbit's ACL tissue

Biomechanical properties of PCL&PET scaffolds

Figure 4 shows the differences in the load-deformation curve between Native ACL, PET&PCL, and PCL. Notably, native ACL has a slight curve and breaks before reaching 5 mm of elongation, while PCL&PET and PCL grafts have longer curved. Moreover, PCL shows higher elongation (< 20 mm) when compared to PCL&PET elongation (>15 mm). However, native ACL has a higher load value (< 150 N) than PCL and PCL&PET load values, which are between 100-150 N. These results suggest that the amount of deformation or stretching is superior in the polymers used in this experiment compared to native ACL, suggesting that PCL is more elastic than PCL&PET grafts.

After tensile testing of PET&PCL and PCL membranes, results were compared with Native ACL tissue of rabbits. N=4 in Native ACL group and N=6 in PCL/PET group. Results taken from Figure 4 (C) show the mechanical properties comparison between Native ACL, bimodal fiber distribution composed of PCL & PET, and bimodal fiber distribution composed of PCL. These results suggest that PCL&PET has mechanical properties similar to native ACL, such as maximum stress 22,72 ± 3.52 N/mm^2 and ultimate strain 1,49 ± 0.36 mm. At the same time, PCL&PET is superior in modulus 3,29 ±0.54 MPa compared to native ACL 1,85 ± 0.8, suggesting that it has good flexibility and is strong enough to resist the compressing forces loaded on the knee.

In contrast to native ACL, the mechanical properties of PCL suggest that it is not flexible enough and has poor biomechanical properties compared to PCL&PET scaffold. In this case, the results show that native ACL can support lower stress when compared to PET&PCL and PCL grafts. While native ACL possesses a maximum stress peak between 30-40 MPa, PCL membrane has a peak less than 2 MPa, and PET&PC graft has a peak > 3 MPa.

Cell proliferation and DNA production.

Figure 5 presents the cell quantification after cell seeding into the scaffolds. DNA proliferation assays were performed in 3 time points (day 0 to day 7). Fibroblast cells were collected from the scaffolds and proceed to process the data after day 7 of cell seeding.

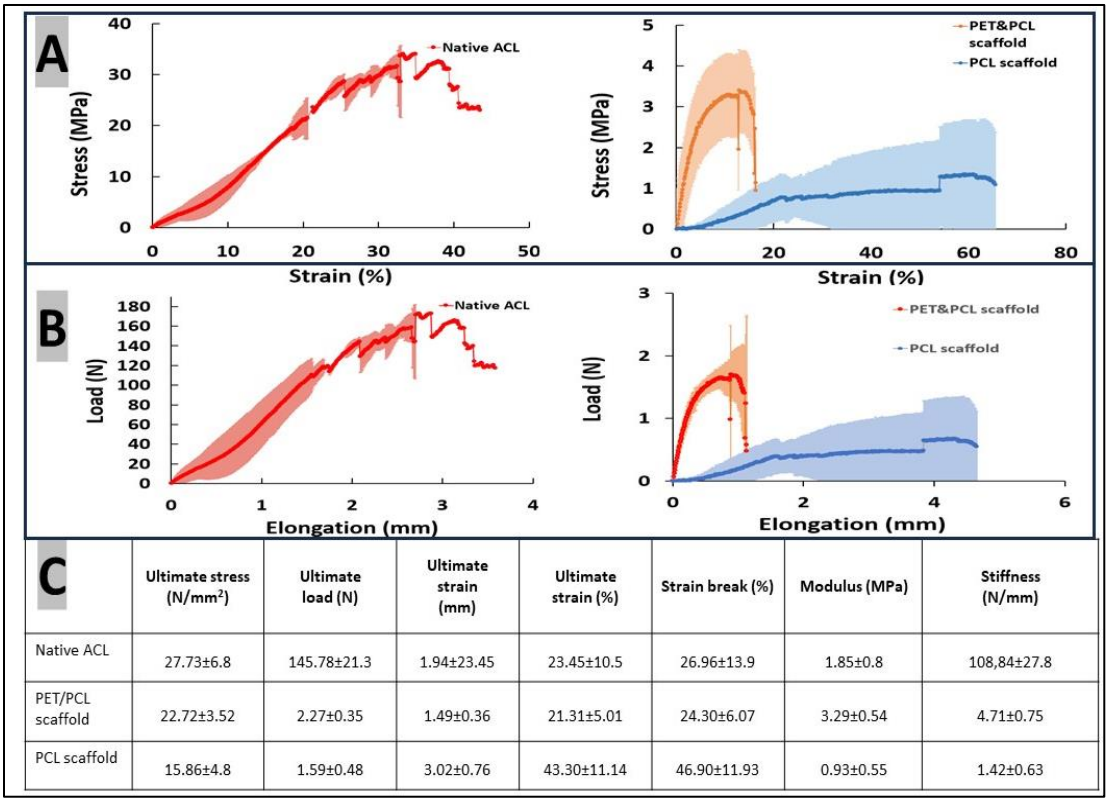

C

	Ultimate stress (N/mm^2)	Ultimate load (N)	Ultimate strain (mm)	Ultimate strain (%)	Strain break (%)	Modulus (MPa)	Stiffness (N/mm)
Native ACL	27.73±6.8	145.78±21.3	1.94±23.45	23.45±10.5	26.96±13.9	1.85±0.8	108,84±27.8
PET/PCL scaffold	22.72±3.52	2.27±0.35	1.49±0.36	21.31±5.01	24.30±6.07	3.29±0.54	4.71±0.75
PCL scaffold	15.86±4.8	1.59±0.48	3.02±0.76	43.30±11.14	46.90±11.93	0.93±0.55	1.42±0.63

Figure 4. Evaluation of the biomechanical properties of collagen ACL fibrils and produced scaffolds from PCL/PET. (A) stress – strain curves. (B) load – elongation curves. (C) Table comparing the values and parameters of A and B. The shaded region in plots show error bars in SD.

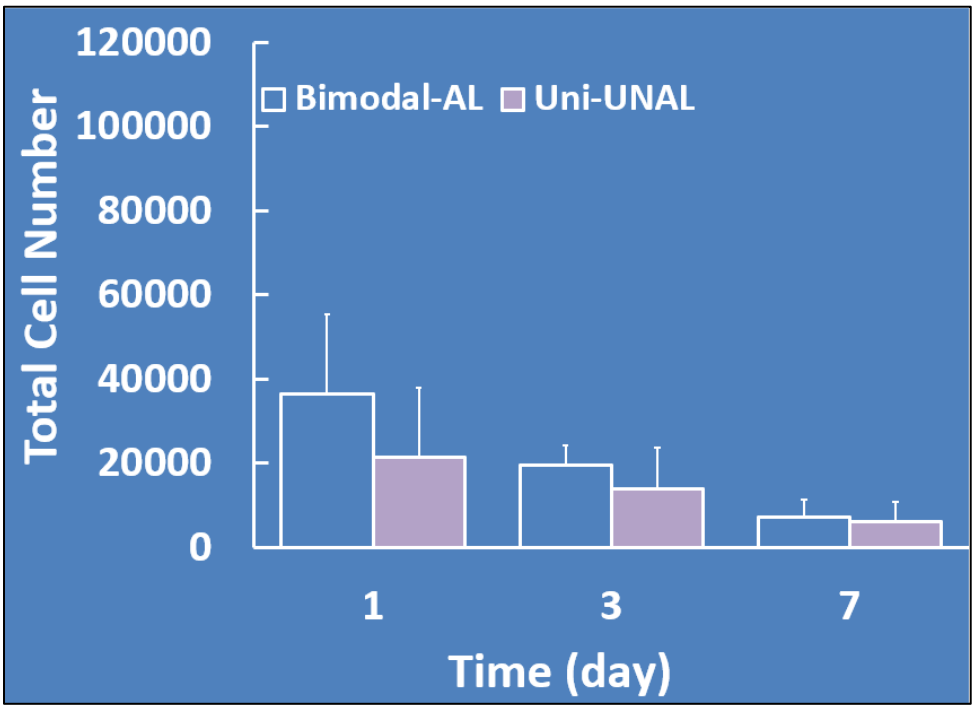

Figure 5. Proliferation of ACL fibroblast (DNA) produced by the cells.

Chapter 4- DISCUSSION

Scaffold production

The results reported here suggest that the produced scaffolds had good quality and are similar in shape, size, and biomechanical characteristics to the ACL tissue of rabbits [31]. The process of making the aligned fiber scaffolds took around 62 hours of electrospinning, and the produced membrane had a thickness of 0.01mm, suggesting that more electrospinning is needed if the thickness needs to be increased. Moreover, the thickness of the membrane could be improved if necessary to increase the biomechanical characteristic of the produced scaffold. On the other hand, the time to produce unimodal fiber distribution scaffold was around 43 hours. It was necessary to have enough membrane to visualize the fiber distribution by SEM, and the produced membrane was used to test the mechanical properties.

Fiber diameter distribution of PCL&PET scaffold

Ligaments, such as the ACL, are known to possess a hierarchical arrangement and consist of collagen fibers of different sizes Within the human ACL, the smallest fibers possess a diameter between 40 and 140 nanometers, while the larger fibrils generally range from 150 to 840 nanometers in diameter [35]. As previously documented, Sheep and rat There were two clear peaks observed in the ACL collagens, one at approximately 100 and 250 nanometers, and another at 60 and 160 nanometers, prior to the injury. However, these peaks transitioned to a single peak at around 100 nm upon damage [36], [37]. Furthermore, some experts claim that the structure of the ACL may undergo alterations as individuals age. However, previous studies on young individuals demonstrated that the primary composition of this ligament is made up of collagen fibers that vary in diameter from 20 to 180 nanometers [38]. In contrast, an earlier study conducted by our team on rabbits has demonstrated that the fiber diameter of ACL tissue varies between 40 and 200 nanometers [39]. The findings of the present investigation revealed that the nanofibers derived from PCL/PET exhibit widths within the range of 40 to 340 nm. In contrast, the unimodal fibers possess a similar peak 125 ± 19.1 nm as injured ACL tissue 112 ± 11 nm.

Biomechanical properties of PCL&PET scaffold

A bimodal distribution enhances the mechanical characteristics by effectively filling the gaps between the larger fibers with smaller fibers, increasing the overall density of the structure. PET, which has exceptional mechanical characteristics, considerably enhanced the tensile strength

of the produced bimodal - aligned scaffold [40]. There was reported a connection between collagen fibers' size distribution and ligaments' mechanical characteristics [41]. Ligaments with a bimodal distribution of fiber sizes tend to have higher tensile properties, while injured ligament tissues typically exhibit a unimodal distribution linked to biomechanical weaknesses [42]**.** The biomechanical tests revealed that the membrane with a bimodal fiber distribution exhibits mechanical properties comparable to those of healthy ACL tissue. Still, the elongation was superior to native ACL in both PCL and PCL/PET cases, suggesting that the polymers can resist more elongation but less load than native ACL. However, native ACL failed at the beginning of the test before reaching 5 mm of elongation, while PCL/PET failed before reaching 15mm and PCL after reaching 15 mm of elongation. The stress-strain curve results suggested that polymeric grafts possess superior tensile strength compared to native ACL. In the case of PCL, it resisted more stress (>4 MPa) compared to PCL/PET (<3 MPA). The polymeric grafts had better mechanical properties in both cases than native ACL, and are more elastic.

Microscopic characterization of PCL&PET scaffolds

Results from microscopic characterization helped to determine the optimal polymeric concentration to obtain bimodal and unimodal fiber distribution. It was required to test different PET concentrations as PCL was quickly acquired by electrospinning it alone and observed by SEM to calculate the fiber diameter. However, in the case of PET, it was more challenging to determine the optimal concentration as the fiber distribution changed every time it was made by electrospinning. In the case of PCL, previous studies helped to determine the optimal concentration for a precise fiber diameter.

Cell seeding and DNA proliferation

Shang et al. evaluated the proliferation of BMSC after seven days, using PET, PET/PCL, and BMP7 loaded with PCL/PET. After seven days, the researchers visualized the cells attached and proliferated in the PCL/PET scaffold loaded with BMP-7 [31]. In contrast, in our study, it is visualized (Figure 5) that the cell number significantly decreased during time. This result was unexpected but can be influenced by many factors, like the growth media used or contamination present in the scaffolds that leads to rapid cell death. To improve the quality of the sterilization process, different cell media for cell growth should be used, and growth factors should be used that could improve the proliferation of primary fibroblasts.

Chapter 5 - CONCLUSIONS

The study demonstrates that the produced scaffolds possess favorable quality, closely resembling the size, shape, and mechanical characteristics of the anterior cruciate ligament (ACL). While additional electrospinning is needed to increase thickness, enhancing thickness could improve the scaffold's mechanical strength [30]. A sufficient membrane for visualizing fiber distribution through SEM was emphasized, even though the produced membrane was not used for testing mechanical properties. These findings highlight the need for further refinement and optimization in scaffold fabrication, focusing on balancing production time, thickness, and mechanical strength.

The mechanical tests revealed that the bimodal fiber distribution membrane demonstrated mechanical characteristics similar to the native ACL. However, the elongation was more significant in both PCL and PCL/PET cases, indicating that the polymers can endure more elongation but less load than the native ACL. The stress-strain curve results further highlighted those polymeric grafts, particularly PCL, exhibited superior tensile strength compared to the native ACL. PCL resisted more stress (>4 MPa) than PCL/PET (<3 MPa). The mechanical properties of the polymeric grafts surpassed those of the ACL tissue. It is important to note that when cells are added to the scaffolds, subsequent tests on the mechanical properties are necessary. This is because the biodegradable nature of PCL can potentially affect the scaffold's tensile strength, load, and stress.

The microscopic characterization was crucial in identifying the optimal polymeric concentration for achieving bimodal and unimodal fiber distribution. For PCL, the process involved electrospinning alone, and SEM observations facilitated the calculation of fiber diameter. However, determining the optimal PET concentration was more challenging due to its tendency to alter fiber distribution with each electrospinning attempt. Previous studies on PCL aided in identifying the optimal concentration for achieving a specific fiber diameter. Moreover, fiber alignment was also achieved to be similar to native ACL rabbit tissue and can be used in future experiments to determine cell migration and alignment into the scaffolds.

Cell seeding experiments showed different results as it was expected. The results obtained by cell seeding into the scaffolds also suggested improving the methods of scaffold assembling sterilization in the future to avoid cell death and to improve cell proliferation.

BIBLIOGRAPHY

[1] J. Anjana, S. Deepthi, K. T. Shalumon, U. Mony, J. P. Chen, and R. Jayakumar, “Nanoengineered biomaterials for tendon/ligament regeneration,” *Nanoengineered Biomaterials for Regenerative Medicine*, pp. 73–93, Jan. 2019, doi: 10.1016/B978-0-12-813355-2.00004-1.

[2] L. M. Cross, A. Thakur, N. A. Jalili, M. Detamore, and A. K. Gaharwar, “Nanoengineered biomaterials for repair and regeneration of orthopedic tissue interfaces,” *Acta Biomaterialia*, vol. 42. Elsevier Ltd, pp. 2–17, Sep. 15, 2016. doi: 10.1016/j.actbio.2016.06.023.

[3] M. Beldjilali-Labro *et al.*, “materials Review Biomaterials in Tendon and Skeletal Muscle Tissue Engineering: Current Trends and Challenges,” 2018, doi: 10.3390/ma11071116.

[4] F. Alshomer, C. Chaves, and D. M. Kalaskar, “Review Article Advances in Tendon and Ligament Tissue Engineering: Materials Perspective,” 2018, doi: 10.1155/2018/9868151.

[5] A. Sensini and L. Cristofolini, “Biofabrication of electrospun scaffolds for the regeneration of tendons and ligaments,” *Materials*, vol. 11, no. 10. MDPI AG, Oct. 12, 2018. doi: 10.3390/ma11101963.

[6] Y. Wu, Y. Han, | Yoke, S. Wong, | Jerry, and Y. Hsi Fuh, “Fibre-based scaffolding techniques for tendon tissue engineering,” 2018, doi: 10.1002/term.2701.

[7] X. Zhang, D. Bogdanowicz, C. Erisken, N. M. Lee, and H. H. Lu, “Biomimetic scaffold design for functional and integrative tendon repair,” *Journal of Shoulder and Elbow Surgery*, vol. 21, no. 2. pp. 266–277, Feb. 2012. doi: 10.1016/j.jse.2011.11.016.

[8] S. L. Y. Woo, J. R. Mau, H. Kang, R. Liang, A. J. Almarza, and M. B. Fisher, “Functional Tissue Engineering of Ligament and Tendon Injuries,” in *Principles of Regenerative Medicine*, Elsevier, 2018, pp. 1179–1198. doi: 10.1016/B978-0-12-809880-6.00067-9.

[9] M. Marieswaran, I. Jain, B. Garg, V. Sharma, and D. Kalyanasundaram, “A review on biomechanics of anterior cruciate ligament and materials for reconstruction,” *Applied Bionics and Biomechanics*, vol. 2018. Hindawi Limited, 2018. doi: 10.1155/2018/4657824.

[10] T. Piontek *et al.*, “Arthroscopically Assisted Combined Anterior and Posterior Cruciate Ligament Reconstruction with Autologous Hamstring Grafts–Isokinetic Assessment with Control Group,” *PLoS One*, vol. 8, no. 12, Mar. 2013, doi: 10.1371/journal.

[11] T. Nau and A. Teuschl, “Regeneration of the anterior cruciate ligament: Current strategies in tissue engineering,” *World J Orthop*, vol. 6, no. 1, pp. 127–136, 2015, doi: 10.5312/wjo.v6.i1.127.

[12] J. A. Cooper, J. S. Sahota, W. J. Gorum, J. Carter, S. B. Doty, and C. T. Laurencin, “Biomimetic tissue-engineered anterior cruciate ligament replacement,” 2007. [Online]. Available: www.pnas.orgcgidoi10.1073pnas.0608837104

[13] B. R. Bach, M. E. Levy, J. Bojchuk, S. Tradonsky, C. A. Bush-Joseph, and N. H. Khan, “Single-Incision Endoscopic Anterior Cruciate Ligament Reconstruction Using Patellar Tendon Autograft Minimum Two-Year Follow-Up Evaluation*,” 1998.

[14] S. B. Lee, Y. H. Kim, M. S. Chong, S. H. Hong, and Y. M. Lee, “Study of gelatin-containing artificial skin V: Fabrication of gelatin scaffolds using a salt-leaching method,”

Biomaterials, vol. 26, no. 14, pp. 1961–1968, 2005, doi: 10.1016/j.biomaterials.2004.06.032.

[15] X. Lu, C. Wang, and Y. Wei, “One-dimensional composite nanomaterials: Synthesis by electrospinning and their applications,” *Small*, vol. 5, no. 21. pp. 2349–2370, Nov. 02, 2009. doi: 10.1002/smll.200900445.

[16] E. Bayrak, B. Ozcan, and C. Erisken, “Processing of polycaprolactone and hydroxyapatite to fabricate graded electrospun composites for tendon-bone interface regeneration,” *Journal of Polymer Engineering*, vol. 37, no. 1, pp. 99–106, 2017, doi: 10.1515/polyeng-2016-0017.

[17] R. Augustine, S. K. Nethi, N. Kalarikkal, S. Thomas, and C. R. Patra, “Electrospun polycaprolactone (PCL) scaffolds embedded with europium hydroxide nanorods (EHNs) with enhanced vascularization and cell proliferation for tissue engineering applications,” *J Mater Chem B*, vol. 5, no. 24, pp. 4660–4672, 2017, doi: 10.1039/c7tb00518k.

[18] C. Y. Tay, S. A. Irvine, F. Y. C. Boey, L. P. Tan, and S. Venkatraman, “Micro-/nano-engineered cellular responses for soft tissue engineering and biomedical applications,” *Small*, vol. 7, no. 10. pp. 1361–1378, May 23, 2011. doi: 10.1002/smll.201100046.

[19] T. L. Jenkins and D. Little, “Synthetic scaffolds for musculoskeletal tissue engineering: cellular responses to fiber parameters”, doi: 10.1038/s41536-019-0076-5.

[20] C. Erisken, X. Zhang, K. L. Moffat, W. N. Levine, and H. H. Lu, “Scaffold fiber diameter regulates human tendon fibroblast growth and differentiation,” *Tissue Eng Part A*, vol. 19, no. 3–4, pp. 519–528, Feb. 2013, doi: 10.1089/ten.tea.2012.0072.

[21] M. Deng, R. James, C. T. Laurencin, and S. G. Kumbar, “Nanostructured polymeric scaffolds for orthopaedic regenerative engineering,” *IEEE Transactions on Nanobioscience*, vol. 11, no. 1. pp. 3–14, Mar. 2012. doi: 10.1109/TNB.2011.2179554.

[22] Z. Ge, J. Cho Hong Goh, and E. Hin Lee, “Selection of Cell Source for Ligament Tissue Engineering,” *Cell Transplant*, vol. 14, pp. 573–583, 2005, [Online]. Available: www.cognizantcommunication.com

[23] H. Liu, H. Fan, S. L. Toh, and J. C. H. Goh, “A comparison of rabbit mesenchymal stem cells and anterior cruciate ligament fibroblasts responses on combined silk scaffolds,” *Biomaterials*, vol. 29, no. 10, pp. 1443–1453, Apr. 2008, doi: 10.1016/j.biomaterials.2007.11.023.

[24] “dunn1993”.

[25] S. R. Caliari and B. A. C. Harley, “The effect of anisotropic collagen-GAG scaffolds and growth factor supplementation on tendon cell recruitment, alignment, and metabolic activity,” *Biomaterials*, vol. 32, no. 23, pp. 5330–5340, Aug. 2011, doi: 10.1016/j.biomaterials.2011.04.021.

[26] B. Veleirinho, F. V. Berti, P. F. Dias, M. Maraschin, R. M. Ribeiro-Do-Valle, and J. A. Lopes-Da-Silva, “Manipulation of chemical composition and architecture of non-biodegradable poly(ethylene terephthalate)/chitosan fibrous scaffolds and their effects on L929 cell behavior,” *Materials Science and Engineering C*, vol. 33, no. 1, pp. 37–46, Jan. 2013, doi: 10.1016/j.msec.2012.07.047.

[27] R. Ng, X. Zhang, N. Liu, and S. T. Yang, “Modifications of nonwoven polyethylene terephthalate fibrous matrices via NaOH hydrolysis: Effects on pore size, fiber diameter,

cell seeding and proliferation," *Process Biochemistry*, vol. 44, no. 9, pp. 992–998, Sep. 2009, doi: 10.1016/j.procbio.2009.04.024.

[28] S. Mohajeri, H. Hosseinkhani, N. G. Ebrahimi, L. Nikfarjam, M. Soleimani, and A. M. Kajbafzadeh, "Proliferation and differentiation of mesenchymal stem cell on collagen sponge reinforced with polypropylene/polyethylene terephthalate blend fibers," *Tissue Eng Part A*, vol. 16, no. 12, pp. 3821–3830, Dec. 2010, doi: 10.1089/ten.tea.2009.0520.

[29] S. A. P. Sughanthy, M. N. M. Ansari, and A. Atiqah, "Dynamic mechanical analysis of polyethylene terephthalate/hydroxyapatite biocomposites for tissue engineering applications," *Journal of Materials Research and Technology*, vol. 9, no. 2, pp. 2350–2356, Mar. 2020, doi: 10.1016/j.jmrt.2019.12.066.

[30] P. Mengsteab *et al.*, "Mechanically superior matrices promote osteointegration and regeneration of anterior cruciate ligament tissue in rabbits," *PNAS*, vol. 46, no. 117, pp. 1–12, 2020, doi: 10.1073/pnas.2012347117/-/DCSupplemental.

[31] P. Zhang, F. Han, T. Chen, Z. Wu, and S. Chen, "'swiss roll'-like bioactive hybrid scaffolds for promoting bone tissue ingrowth and tendon-bone healing after anterior cruciate ligament reconstruction," *Biomater Sci*, vol. 8, no. 3, pp. 871–883, Feb. 2020, doi: 10.1039/c9bm01703h.

[32] F. Han, P. Zhang, Y. Sun, C. Lin, P. Zhao, and J. Chen, "Hydroxyapatite-doped polycaprolactone nanofiber membrane improves tendon–bone interface healing for anterior cruciate ligament reconstruction," *Int J Nanomedicine*, vol. 10, pp. 7333–7343, Dec. 2015, doi: 10.2147/IJN.S92099.

[33] J. A. Parry *et al.*, "A Combination of a Polycaprolactone Fumarate Scaffold with Polyethylene Terephthalate Sutures for Intra-Articular Ligament Regeneration," *Tissue Eng Part A*, vol. 24, no. 3–4, pp. 245–253, Feb. 2018, doi: 10.1089/ten.tea.2016.0531.

[34] S. Wang *et al.*, "Enhance the biocompatibility and osseointegration of polyethylene terephthalate ligament by plasma spraying with hydroxyapatite in vitro and in vivo," *Int J Nanomedicine*, vol. 13, pp. 3609–3623, Jun. 2018, doi: 10.2147/IJN.S162466.

[35] L.-H. Yahia and G. Drouin, "Collagen structure in human anterior cruciate ligament and patellar tendon," 1988.

[36] A. O. Adeoye *et al.*, "A biomimetic synthetic nanofiber-based model for anterior cruciate ligament regeneration.," *Front Bioeng Biotechnol*, vol. 10, p. 969282, 2022, doi: 10.3389/fbioe.2022.969282.

[37] S. Smatov, "Polycaprolactone based nanofiber scaffolds can mimic collagen fibril diameter distribution of healthy and injured sheep Anterior Cruciate Ligament," 2021.

[38] R. Strocchi, V. De Pasquale, A. Facchini, M. Raspanti, S. Zaffagnini, and M. Marcacci, "Age-related changes in human anterior cruciate ligament (ACL) collagen fibrils," *Ital J Anat Embryol*, vol. 101, no. 4, p. 213—220, 1996, [Online]. Available: http://europepmc.org/abstract/MED/9203869

[39] S. Kadyr *et al.*, "Braided biomimetic PCL grafts for anterior cruciate ligament repair and regeneration," *Biomedical Materials (Bristol)*, vol. 19, no. 2, Mar. 2024, doi: 10.1088/1748-605X/ad2555.

[40] J. Brand, A. Weiler, D. N. M. Caborn, C. H. Brown, D. L. Johnson, and § Md, "Current Concepts Graft Fixation in Cruciate Ligament Reconstruction," 2000.

[41] C. Niyibizi, K. Kavalkovich, T. Yamaji, and S. L. Y. Woo, “Type V collagen is increased during rabbit medial collateral ligament healing,” *Knee Surgery, Sports Traumatology, Arthroscopy*, vol. 8, no. 5, pp. 281–285, 2000, doi: 10.1007/s001670000134.

[42] K. Shino, B. W. Oakes, S. Horibe, K. Nakata, and N. Nakamura, “Collagen Fibril Populations in Human Anterior Cruciate Ligament Allografts Electron Microscopic Analysis*,” 1993.